Wetland hydrodynamics and mitigation of pesticides and their metabolites at pilot-scale

Celine Gaullier, Nicole Baran, Sylvie Dousset, Nicolas Devau, David Billet, Geraldine Kitzinger, Emeline Coisy

Wetland hydrodynamics and mitigation of pesticides and their metabolites at pilot-scale

Céline Gaullier [1, 2, 3], Nicole Baran [2], Sylvie Dousset *[1, 3], Nicolas Devau [2], David Billet [1, 3], Géraldine Kitzinger [1], Emeline Coisy [2]

[1] Université de Lorraine - CNRS - Laboratoire Interdisciplinaire des Environnements Continentaux - 54506 Vandœuvre-lès-Nancy, France

[2] BRGM - 45060 Orléans CEDEX 02, France

[3] LTSER France, Zone Atelier du Bassin de la Moselle - 54506 Vandœuvre-lès-Nancy, France

*Corresponding author:

Sylvie DOUSSET

LIEC - Université de Lorraine - CNRS

BP 70 239

54 506 Vandœuvre-lès-Nancy Cedex, France

Tel: (+33) 03 72 74 52 12

sylvie.dousset@univ-lorraine.fr

ABSTRACT

Constructed wetlands (CWs) are useful for reducing pesticide transfer from drainage into surface water, though little was known about the influence of hydrodynamics on their mitigation. We thus assessed the influence of design parameters (aspect ratio, water depth, flow rate) on hydraulic performance simultaneously to pesticide mitigation. We performed our work on four pesticides with contrasted properties: boscalid (BSC), cyproconazole (CYP), isoproturon (IPU) and dimethachlor (DMT), under three controlled flow-rate conditions (including no-flow) by using two pilots with contrasted designs (pond and ditch) over 62 days. Hydraulic performance and pesticide mitigation were less effective in a pond than in the ditch whatever the flow. Moreover, pesticide mitigation was more significant at low than at high flow rates for both pilots. At high flow rate, water transport is mainly governed by convection, but at low flow rates both water transport and mitigation are governed by hydrodynamic dispersion, inducing a longer contact time between pesticides and substrate due to longer hydraulic retention. Finally, BSC and CYP are better mitigated than DMT and IPU, even if they are also more strongly released during low flow rates. In addition, the mitigation of pesticides and some of their metabolites produced inside the pilots was almost complete during stagnation.

Keywords: constructed wetland; flow rate; hydraulic performance; pesticide; remediation; water tracer

1. Introduction

In order to protect and improve water quality (JOCE, 2000), the use of Free Water Surface Constructed Wetlands (FWS CWs) with tile drains at about 1-m depth has emerged as a cost-effective way of reducing contaminant loading from drainage waters (Schultz et al., 1995; Moore et al., 2001; Tournebize et al., 2012; Vallée et al., 2015b). Their effectiveness in mitigating pesticide concentrations has been demonstrated in several studies (Moore et al., 2001; Wilson et al., 2011; Elsaesser et al., 2011), but locally negative mitigation rates have been reported as well depending on molecules and hydrological year (Passeport et al., 2013; Maillard and Imfeld, 2014; Vallée et al., 2015b). A review of 47 studies covering 87 reveals average removals varying from 97 to 24% according to pesticide physicochemical parameters (Vymazal and Březinová, 2015). For both controlled and uncontrolled flow in CW, average retention efficiencies for pesticide are similar (32-39%) but the performance is highly variable dependent on hydrological conditions and seasons (Tournebize et al. 2017). Indeed, several parameters are known to affect the hydraulic effectiveness of CWs, such as (i) the length-to-width ratio (LWR) of the wetland, and (ii) the hydraulic residence time (HRT), flow rate and water depth, but the influence of these hydraulic parameters on pesticide mitigation has rarely been studied (Blankenberg et al., 2007; Boutron et al., 2011; Elsaesser et al., 2011; Haarstad and Braskerud, 2005; Vallée et al., 2015a).

HRT is considered as one of the main factors influencing the mitigation effectiveness of CWs (Stehle et al., 2011; Vyzamal and Březinová, 2015; Guo et al., 2017); it is mainly controlled by the flow path through the wetland, inflow rate, and water depth. From field experiments, the influence of HRT on pesticide mitigation is not very clear (Maillard and Imfeld, 2014; Vallée et al., 2015b), but some studies carried out under controlled conditions reported an increased effectiveness with a longer HRT (Elsaesser et al., 2011; Vallée et al., 2015a). These authors tested HRTs ranging from 4 hours to 7.4 days, corresponding to inflow rates ranging from 3.2 $L.s^{-1}$ to 0.05 $L.s^{-1}$ (Holland et al., 2004; Elsaesser et al., 2011; Vallée et al., 2015a; Maillard et al., 2016), which can be assimilated to low flow rates in the field, where flow rates can range from 0.01 to 20 L/s (Larson et al., 2000; Vallée et al., 2015b). However, the effectiveness of high flow rates coupled with very short HRTs (a few hours) was rarely studied under controlled conditions, even though they may represent about 50% of drainage flow over one year in the field (Tournebize et al., 2013; Vallée et al., 2015b). In addition, flow rate and water depth both affect wetland hydraulics (Holland et al., 2004) by changing the effective volume that can be used for pollutant mitigation, and the length-to-width ratio (LWR) seems to be a major factor in determining the effectiveness of a CW by controlling flow uniformity (Thackston et al., 1987; Su et al., 2009); these authors showed that the mitigation effectiveness of a CW is considered as satisfactory for a LWR between 1.8 and 10.

Our study is one of the first to investigate the influence of highly contrasted flow rates on the flow patterns of hydraulic zones in CWs, and their impact on pesticide mitigation. For that purpose, laboratory experiments were carried out on two pilot-scale wetlands with different designs under variable hydrodynamic conditions, studying four pesticides—boscalid (BSC), cyproconazole (CYP), isoproturon (IPU) and dimethachlor (DMT)—with contrasted polarities. Such a controlled small-scale approach, compared to an *in-situ* study, is required for understanding the parameters and processes controlling pesticide mitigation in CWs. The experiments were conducted by associating two conservative tracers (chloride and bromide) with the four pesticides during a drainage period with alternating high-, low- and zero flow.

2. Material and Methods

2.1. Pilot set-up

Two laboratory pilot installations, both mimicking field CWs, were constructed in polyvinylchloride. Soils and sediments were sampled in field CWs, dried for one week at 24 °C, crushed and sieved at 2 mm, and then homogenized. Their main characteristics are provided in Table A.1. The first pilot reproduced a ditch-shaped CW at Manoncourt-sur-Seille (France) at 1:40 scale, using 22 kg of soil from this site deposited with a thickness of 3 cm and covered with 360 g of sediment over 0.5 cm thick. It was 225 cm long and 2.5 cm wide, with an enlarged section of 25 x 6.5 cm. The vegetation, grown from seeds in the soil, was dominated by *Juncus effusus, J. bufonius* and grasses on the edges of the pilot that not affected flow) (Fig. 1).

The second pilot simulated a CW formed by a succession of three ponds at Ville-sur-Illon (France) at 1:20 scale, using 55 kg of soil from the site deposited with a thickness of 5 cm and covered with 2 kg of sediment over 0.5 cm thick. It was 235 cm long and 20-30 cm wide, depending on the ponds, with an island (15 x 7 cm) at the beginning of the second pond, as in the field. The vegetation, again developed from seeds in the soil, was dominated by *Juncus effusus, J. inflexus and J. articulatus* on the pond edges (not affecting flow), and by *Typha latifolia* and *Veronica becabunga* inside the ponds (Fig. 1). The detailed dimensions of the pilots are given in Table A.2. Both ditch and pond CWs were chosen for their contrasted design and their simplicity of laboratory implementation, in order to reproduce their use for large-scale pesticide mitigation.

Before running the experiments over a 62-day period, both pilots were left during 8 months for stabilization and plant growth, and were watered by tap water. Operating conditions in the phytotronic room were 20±2 °C, with a day/night ratio of 14/10 h, a hygrometry of 70% and a brightness of 3100 to 3800 lx.

2.2. *Selected pesticides*

Four pesticides were selected on the basis of their actual field application, their detection in the water of existing CWs, and the diversity of their polarities (Octanol-water partition coefficient from 148 to 1230) or sorption coefficient K_{OC} from 69 to 772 $L.kg^{-1}$). The selected pesticides were the two fungicides *boscalid* (2-chloro-N-(4'-chloro[1,1'-biphenyl]-2-yl)pyridine-3-carboxamide) and *cyproconazole* (α-(4-chlorophenyl)-α-(1-cyclopropylethyl)-1*H*-1,2,4-triazole-1-ethanol), and the two herbicides *isoproturon* (*N*,*N*-dimethyl-*N*'-(4-(1-methylethyl)phenyl)urea) and *dimethachlor* (2-chloro-*N*-(2,6-dimethylphenyl)-*N*-(2-methoxyethyl)acetamide). Their main properties are given in Table A.3. The analytical standards of these pesticides were purchased from Cluzeau (Sainte-Foy-La-Grande, France). All four were analytical standard grade (>98 %) and are used both for spiking and confirmation. The analytical standards of the IPU and DMT metabolites (see Table A.4) were purchased from Restek (Lisses, France), Sigma (Lyon, France), Neochema (Bodenheim, Germany) and Techlab (Metz, France).

2.3. Simulated drainage, stagnation and tracing

In order to mimic real conditions, the experimental flow rates were determined based on *in situ* observations. In the field, flow-rate monitoring (with an ultra-sound flowmeter, 950-US 50 Hz, SIGMA) over one year indicated that 90% of the flow values varied from 0 to 4 $L.s^{-1}$ and 10% varied from 4 to 10 $L.s^{-1}$ for the ditch (D) CW. For the pond (P) CW, 70% of the flow values varied from 0 to 5 $L.s^{-1}$, 10% varied from 5 to 10 $L.s^{-1}$ and 20% varied from 10 to 18 $L.s^{-1}$. In addition, a stagnation period (zero flow) also occurred after a drainage event.

Based on these field observations, we applied two distinct inflow rates to each pilot, calculated according to the pilot scales of 1:40 and 1:20. The high inflow rates were

7.0 mL.min^{-1} for the ditch pilot (D-HF) and 55.5 mL.min^{-1} for the pond pilot (P-HF), corresponding to field scales of 7.5 and 7.4 L.s^{-1}. These values are representative of the high and medium inflow rates defined for ditch CW and pond CW, respectively. Thus, for the high flow rate, the nominal HRTs (i.e. the wetland-volume/flow-rate ratio) were 4.0 and 2.8 h for ditch pilot and pond pilot, respectively. This agrees with the HRTs measured in the field at high flow (about 30 min to 6 h). The low inflow rates were 1.8 and 8.0 mL.min^{-1} for ditch pilot (D-LF) and pond pilot (P-LF), respectively, corresponding to field values of 1.9 and 1.1 L.s^{-1}, respectively. The nominal HRTs were 11.0 and 9.8 h for the ditch and pond pilots, respectively; these values have the same order of magnitude as the HRTs measured in the field at low flow (about 8 to 60 h). A drainage event was simulated during 12 h for a high inflow rate and during 36 h for a low inflow one, corresponding for each flow rate condition to at least three nominal HRTs in the pilot. Subsequently, a stagnation period (no-flow) was simulated for 50 days to represent a long *in-situ* period of stagnation (i.e. almost three months in summer). During this step, to balance evapotranspiration, the water depth was maintained at 1 cm and 1.5 cm, respectively for the ditch and the pond pilots, by adding distilled water twice a day.

Drainage inflow was injected continuously through Teflon tubing (AJD00017, Saint Gobain, France) using a peristaltic pump (Ismatec IPS-16). The water inlet and outlet were located in the middle of each pilot. The simulated drainage was divided into eight consecutive charge and discharge steps (S1 to S8) (Table 1). BSC, CYP, IPU and DMT were injected with a concentration of 200 µg.L^{-1} at the same time as water-tracer ions at 11.5±1.5 mg.L^{-1} during the S1 and S3 charge steps, and distilled water was injected during the S2, S4, S5 and S8 discharge steps. The tracers used were chloride ($CaCl_2$) during the S1 step (high flow) and bromide (KBr) during the S3 step (low flow), for determining the mean (real) HRT and for measuring the hydraulic efficiency. No loss of ions and pesticides was observed in the inlet solution. Moreover, the first high inflow charge (S1) was done in a half-full pilot, i.e. in the field the CW was not dry when drainage started.

In addition, a brilliant blue (BB) dye tracer at 0.05 mg.L^{-1} was continuously injected after discharge S8. Pictures were automatically taking each minute for D-LF, and each 30 sec for D-HF, P-HF and P-LF, to monitor the water pathways.

2.4. Sampling strategy

During the drainage periods (S1 to S5 and S8), outlet effluents were continuously collected through a Teflon tube (AJD00017, Saint Gobain, France) with a peristaltic pump (Ismatec IPS-16); they were stored in polyethylene flasks using a fraction collector (Foxy 200^{TM}). At high flow (S1-S2-S4), automatic samples were taken every 15 min during the first 3 h and then every hour for the following 9 h. At low flow (S3-S5-S8), automatic samples were taken every 30 min during the first 6 h and then every 3 h for the following 30 h, and over the next 6 days for the S8 steps. All samples were stored less than 12 h in the polyethylene flasks (pesticide loss from 1 to 5% in the flasks, determined in triplicate at 200 µg.L^{-1}) and then stored in glass tubes. Moreover, all samples were individually analysed within 24 hours.

In addition, 5 mL water samples were collected manually inside the pilots in two specific zones (SZ) (Fig. 1), every 3 h at high flow (S1-S2-S4), and every 9 h at low flow (S3-S5-S8) for the two pilots (4 samples). During the S7 stagnation period, composite (6 x 1 mL) samples representative for the pilot were taken in the same place, daily for the first 10 days, and then after 12, 14, 16, 18, 20, 26, 32, 38, 44, 50 days of stagnation.

Finally, at the end of the experiment, after emptying the pilots, soil and plants were freeze-dried, manually crushed and homogenized, before bromide and pesticide extraction and analysis.

2.5. *Pesticide analyses*

For each water sample, 2 mL was placed in a PP 2 mL centrifuge tube and then centrifuged at 16,873 *g* for 5 min to eliminate any suspended particles (i.e. to investigate the mitigation on the dissolved phase only). Then, a 1 mL aliquot was transferred to an amber glass vial for pesticide analysis within 24 h after sampling (Method A). Finally, part of the centrifuged sample was frozen at -20 °C to analyse for IPU and DMT metabolites (methods B and C) and analysis within 2 months.

Method A was performed by liquid chromatography (LC) using an Ultimate 3000 RSLC system and a Diode Array Detector (Gaullier et al., 2018), analysing BSC, CYP, IPU and DMT. Methods B and C were done in an Acquity Ultra-Performance LC system (UPLC, Waters), interfaced to a triple quadrupole mass spectrometer (Quattro Premier XE, Waters). Method B analysed for mono-desmethyl-IPU (MD-IPU), di-desmethyl IPU (DD-IPU), and the DMT metabolites CGA 39981 and CGA 42443. Method C analysed for the DMT metabolites CGA 42443 (DMT-OA), CGA 354742 (DMT-ESA), CGA 369873, CGA 373464, SYN 530561 and SYN 528702. The three analytical methods are described in further detail in the Appendices.

The pesticides were only extracted from the sediments (not from plants) by a modified QuEChERS (Quick, Easy, Cheap, Effective, Rugged and Safe) method described in the Appendices (Fernandes et al., 2013) before analysing them with Method B, the LOQ being 0.0005 $\mu g.g^{-1}$ for BSC, 0.0002 $\mu g.g^{-1}$ for CYP and DMT, and 0.0001 $\mu g.g^{-1}$ for IPU. The values were corrected by the extraction yield of the QuEChERS method: 88.3 ± 0.7%, 70.2 ± 3.8%, 74.0 ± 4.4% and 106.8 ± 1.9% for BSC, CYP, DMT and IPU, respectively.

2.6. Ionic tracer analysis

Each water sample was filtered through a 0.22 µm cellulose acetate filter and then a 1 mL aliquot was transferred to a polypropylene vial for analysis with a Dionex ICS-3000 ion-chromatographic instrument (Sunnyvale, CA, USA), using Chromeleon® software (Version 6.80) to determine Cl^- and Br^- concentrations. The analytical method is described in the Appendices. In addition, at the end of the experiment the bromide tracer was extracted from 10 g of sediment with a $CaCl_2$ solution (10 mL – 10^{-4} M) and from 0.8 g of plant material with distilled water (80 mL), by stirring for 40 min, and then analysed.

2.7. Data analysis

2.7.1. Water transport parameters

The residence time distribution (RTD) function, E(t), is defined mathematically such that E(t)×dt is the fraction, at the outlet, of fluid that has spent between t and t+dt time in the flow system (Adeosun and Lawal, 2009). In order to compare the RTDs for our four studied conditions (D-HF, D-LF, P-HF and P-LF), each RTD must be normalized. The normalized hydraulic retention time (HRT) (t_Θ), was defined as the ratio between the mean HRT (t_{mean}) and the nominal HRT (t_n) (Fan et al., 2008). In order to estimate the hydraulic performance of the pilots, the normalized HRT (t_Θ), the normalized variance (σ_Θ), the number of cells (N) and the hydraulic efficiency (λ) were determined. The detailed calculation is given in the Appendices. The hydraulic performance is considered as good when all these parameters are optimized, such as when the water is transported from inlet to outlet throughout the entire volume system, limiting short-circuits.

2.7.2. Restitution of tracer ion and pesticide mitigation rate

The restitution percentage of each tracer was calculated according to Equation (1):

$$restitution = \frac{Q_{out}}{Q_{in}} \times 100 \qquad (1)$$

where Q_{in} is the total amount injected (mg) and Q_{out} is the total amount outlet (mg) defined by Equation (2).

$$Q_{out} = \sum_0^{\infty} C(t)\,V(t) \qquad (2)$$

where C(t) ($mg.L^{-1}$) is the outlet concentration at each time step and V(t) (L) is the outlet volume at each time step.

The effectiveness (%) of the pilots to mitigate pesticides was also calculated with Eq. (1) and (2), replacing the ion tracer by pesticides mass.

2.7.3. Dissipation and degradation of pesticides

Pesticide dissipation kinetics in water during the stagnation period were described using a second-order model before calculating the associated half-live DT_{50} was calculated (see Appendices).

The dissipation of pesticides can partly be due to their degradation. The rate of degradation (ratio between the molar concentrations of metabolites and parent molecule) was estimated for each metabolite during (i) the drainage period and ii) the stagnation period.

2.8. Statistical analysis

First, the hydraulic variables used for defining the drainage period in the two pilot systems were converted into categorical (discrete) variables. The semi-quantitative values measured for the volume- and hydraulic-efficiency- variables were divided into four ranks; another three ranks were defined for the flow-rate variable, and HRT and the LTW values were aggregated into two more ranks (Table A.5). The ranking groups were defined beforehand.

Of the variables used for describing the pesticide properties (DT_{50} water, K_d, P_{max}, discharge) except the T_{eq} variable, the quantitative values were also transformed into categorical (discrete) variables. To this end, a unimodal distribution was calculated for each variable after centring and scaling all data. After that, first and third quartiles as well as the median were defined. Based on these values, four ranks were defined for each variable. The first corresponds to values below the first quartile, the second is for values ranging between the first quartile and the median, the third rank consists of values ranging between the median and the third quartile, and the fourth rank aggregates the values above the third quartile. For the T_{eq} variable, five ranks are considered.

Multiple correspondence analysis (MCA) then ordered the 16 observations according to the hydraulic and pesticide variables used for their definition. The Φ^2 distance-based matrix was calculated from re-organized data according to a Burt table. The results were displayed as a symmetric plot showing both variables and observations along the first two principal axes. Based on the Φ^2 distance-based matrix associated with Ward's method for aggregating data, an agglomerative hierarchical principal-component clustering (HCPC) was calculated and the first four principal components then were used for constructing the associated dendrogram. The dendrogram tree was then cut into several groups based on the higher relative loss of inertia criteria, allowing the aggregation of observations into classes.

Finally, a partial least squares discriminant analysis (PLS-DA) discriminated observations among the groups defined from the HCPC analysis. To this end, multivariate analysis computed the best discriminant functions for differentiating objects in groups while maximizing variance between treatments, though minimizing intra-variance for which the first four main axes from the MCA calculations were used. This analysis is based on a partial least squares regression algorithm that searches for latent variables with maximum covariance and represents the relevant sources of data variability with linear combinations of the original variables (Ballabio and Consonni, 2013). The results were presented as a correlation circle of variables, distributing the sixteen observations along the two discriminant axes. A confusion matrix, comparing the *a priori* (real) and *a posteriori* (calculated) classification of the observations, was calculated as well with the cross-validation technique. All statistical tests were carried out using FactoMineR and ade4 R-software.

3. Results and discussion

3.1 Influence of pilot design parameters and flow rate on hydrodynamic

Table 2 shows the water-transport parameters derived from RTD data. For high flow (HF) or low flow (LF), both ditch and pond have quite similar t_{mean} and v_{mean} values, indicating that water-residence time and water velocity were roughly the same for both pilots. However, σ^2_Θ was lower for ditch than pond and *N* was higher, indicating that the ditch behaved more like a plug-flow, whereas the pond behaved as a mixing system (Fan et al., 2008). In addition, σ was greater for pond than ditch, indicating a greater dispersion of water in the pond compared to the ditch, probably toward the borders, due to its larger width. Moreover, the hydraulic efficiency (λ) was higher for the ditch than for the pond. Thus, all parameters indicated that the hydraulic performance was higher for ditch than pond, regardless of flow rate. This could be due to the morphology and dimensions of both pilots: as the length-to-width ratio for ditch is five times higher than for pond, an optimal water-flow path is induced in the ditch pilot as suggested by other authors (Thackston et al., 1987; Haarstad and Braskerud, 2005; Su et al., 2009).

For both pilots, the t_{mean} at LF (22 h) is higher than that at HF (4-5 h), indicating that the water spends a longer time in the pilot when the flow rate is lower (Table 2). In addition, for both pilots, the hydraulic efficiency λ and the effective volume (e_v) were higher at LF than at HF. Moreover, e_v was >1, probably indicating a storage zone in both pilots, especially at LF and probably due to greater dispersion of water. This assumption was confirmed by (i) a greater σ at LF than at HF, (ii) a more dispersed progression front of the BB dye at LF than at HF, and (iii) similar ionic-tracer concentrations at the outlets and in specific zones at HF, which are different at LF (Fig. A.1). Thus, water-transport parameters indicated that the hydraulic performance was higher at LF than at HF for both pilots, which might be due to distinct water-transport mechanisms inside the pilot, depending on flow rate. At HF, the transport was dominated by convection in the main channel, while at LF the transport was also governed by hydrodynamic water dispersion (including molecular diffusion and kinematic dispersion) from the main channel into the whole pilot volume, convection still occurring in the main channel (Gaullier et al., 2018; Holland et al., 2004).

3.2 Influence of hydrodynamics on pesticide mitigation

Tracer recoveries were over 90% at the end of the experiments (Fig. 2). Regardless of the studied flow rate and pesticides, the pesticide-export rate at the outlet (charge + discharge) was lower for the ditch (49.1 to 86.9%) than for the pond (78.8 to 99.4%) (Fig. 2), indicating a better mitigation through the ditch. Its higher mitigation could be due to the lower water depth (at LF 1 cm and 1.5 cm in ditch and pond, respectively, and at HF 1.5 cm and 3 cm in the same pilots), which enhances the surface contact with sediments and increase the adsorption (Gaullier et al., 2018). Regardless of the studied pilots and pesticides, the exported rates at the outlet (charge + discharge) for the four pesticides were lower at LF (49.1 to 87.1%) than at HF (66.2 to 99.4%) (Fig. 2). This result agrees with those reported under controlled conditions by other authors (Boutron et al., 2011; Moore et al., 2013; Vallée et al., 2015a). Thus, pesticide mitigation is higher at LF than at HF, probably associated with a longer residence time as well as with water-transport mechanisms governed by hydrodynamic dispersion and convection at LF, whereas at HF only convection is the main process of water transport.

For both flow rates, during charge phases (S1 and S3), the exported rate of pesticides was lower than that of ionic tracers in the ditch, indicating pesticide retention and/or degradation inside the pilots. According to their mitigation, pesticides can be classified as BSC > CYP > DMT ≥ IPU, which is consistent with their adsorption coefficient and suggests that retention could be a major process (Gaullier et al., 2018; Vymazal and Březinová, 2015, Tournebize et al. 2017). Note, however, that the mitigation we observed is lower than those mentioned by Tounebize et al. (2017). According to their classification IPU and DMT belong to group I (average of 25% of removal efficiency, BSC to group II – 49% and CYP to group III -51 %). In the pond, however, the exported rate of pesticides was almost similar to that of ionic tracers, indicating that pesticides travelled freely in the water with few interactions with substrates except for BSC having the highest adsorption coefficient.. Taking into account the discharge phases (S2 and S4+S5), the exported rate was similar for all pesticides and both pilots during HF conditions. During LF, however, it was higher for pond than for ditch. Moreover, BSC and CYP had higher exported rates than DMT and IPU, especially during LF discharge (S5), as previously shown in a pilot-scale experiment by Vallée et al. (2015a). Thus, for HF, the pesticides not adsorbed on sediment during charge step (S1) are released during the following discharge step (S2) due to convective flux. At LF, however, the rate of exported pesticides could be due to both convective and dispersive flux and pesticide desorption from sediment and vegetation, especially for BSC and CYP. Indeed, the amount of released ionic tracer (i.e. not adsorbed) was lower than that of released BSC and CYP, especially for the ditch pilot, indicating that desorption reactions may occur. In addition, a higher percentage of metabolites was recovered at LF (0.5-1.4% of initial IPU and 0.4-0.9% of initial DMT) than at HF (0.2-0.6% of initial IPU and 0.03-0.13% of initial DMT) (Fig. A.2). A low flow-rate highlights differences that are related to molecular properties, probably due to the longer retention time that also promotes slower processes, such as degradation or desorption.

Finally, the HCPC test aggregated the sixteen observations in four groups corresponding to the four studied conditions: pond-HF (obs. 1-4), pond-LF (obs. 5-8), ditch-HF (obs. 9-12) and ditch-LF (obs.13-16) (Figs 3). The PLS-DA statistical test (fig 3D) highlights the important factors in pesticide mitigation. The first (F1=57.27%) and second (F2=35.18%) discriminant axes describe with a high degree of confidence (F1+F2 represent 90% of variance) the distribution of the four classes determined from the sixteen observations (Fig. 3). The four groups determined from HCPC analysis are all separated by discriminant axis 1, which was mainly based on the first principal axis calculated from the MCA that is itself based on the four hydraulic parameters of flow rate, water depth, pilot volume and hydraulic efficiency. In addition, the groups are separated by the second discriminant axis, calculated based on the third principal MCA-derived axes. This third principal component is mainly related to pilot volume and hydraulic efficiency. Observations 1 to 4 and 13 to 16 are located in the upper part of the scatter plot and are discriminated from observations 5 to 12 according to the second discriminant (Fig. 3). These results show that the observations with higher pilot volume and hydraulic efficiency (observations 1-4 and 13-16) are clearly discriminated from the others. The MCA results show that hydraulic variables contributed more strongly to the principal axes than the pesticide-related variables, indicating that the classes calculated from HCPC are strongly dependent upon the hydraulic variables. The high variance associated with the PLS-DA confirms that hydraulic variables (flow rate, water depth, volume and hydraulic efficiency) are suitable for group observations. The group showing higher pesticide mitigation is associated with lower flow rates, water depth and volume. These results agree with observations by others authors (Holland et al., 2004; Boutron et al., 2011; Moore et al., 2013), even if the results were contradictory for flow rates (Holland et al., 2004; Moore et al., 2013). Flow rate and volume conditions were different for a similar HRT (due to pilot morphology), indicating that hydraulic parameters have a stronger influence on pesticide mitigation than the HRT. Combining MCA and PLS-DA analyses shows that pesticide-related variables (K_d, $DT_{50\text{-water}}$) contribute mainly to intragroup variance. In addition, the small size of the data set implies that one observation is associated with only one pesticide. Therefore, the difference of pesticide mitigation according to their physico-chemical properties could not be correctly determined from our dataset. One way to overcome this limit would be to repeat part of the experiments, especially the LF experiments where mitigation is higher, several times to obtain multiple observations associated with each tested pesticides.

3.3 Mitigation of pesticides during a no-drainage period followed by discharge

Regardless of pilot and molecules, the water DT_{50} values, ranging from 0.5 to 1.2 days showed fast dissipation of pesticides from the aqueous phase, as earlier shown for IPU and BSC (Vallée et al., 2015a) (fig. 4). The DT_{50} values are generally lower or equivalent in the pond than in the ditch (0.5 vs. 0.8 for BSC, 0.6 vs. 1.1 for CYP, 0.8 vs. 1.2 for IPU and 0.7 vs. 0.7 for DMT). Consequently, after 50 days of stagnation, less than 1% and 0.5% of the four pesticides remained in the ditch and pond waters, respectively. The decrease in IPU and DMT concentrations was accompanied by a simultaneous increase in metabolite concentrations (Fig. 4B and 4C) during the first ten days of stagnation, testifying to a degradation of these molecules during the experiment.

After 50 days of stagnation, the two IPU-metabolite concentrations in water were less than LOQ, whereas a small amount of DMT metabolites remained in water notably DMT-OA. For the two pilots, at least 5% of the IPU was degraded into metabolites after 50 days, in accordance with IPU degradation rates determined elsewhere in water: 1.6-2.2% (160-200 days) (Rönnefahrt et al., 1997) and 3.5-35% (50 days) (Vandermeeren et al., 2016). The concentration peak of the metabolite MD-IPU was 9 and 4.5 times higher than that of DD-IPU (for ditch and pond, respectively), indicating that IPU is preferentially degraded into MD-IPU as earlier shown (Rönnefahrt et al., 1997). Regarding the degradation of DMT in the ditch, about 17.5% was degraded into DMT-OA, CGA 42443, DMT-ESA, CGA 39981 or CGA 373464, and in the pond about 35% was degraded into DMT-OA, CGA 39981 (higher amount), CGA 42443, DMT-ESA or SYN 528702 (Fig. 4C). We noticed that the ratios between DMT metabolites are pilot-dependant with a prevalence of DMT-OA and CGA 39981 vs. DMT-ESA in the pond during the first days while the three metabolites are similar concentrations in the ditch. As our study is the first to provide information on DMT metabolites, we could not compare our results to previous data.

During the last 7-day step with low-flow discharge (S8) following the stagnation period, the four pesticides were quantified at higher concentrations than at the end of stagnation step (S7), indicating that they may have been desorbed from sediment and/or plants. As observed during drainage and in both pilots, BSC and CYP are more released into water (0.9–1.8% of the initial injected amount in S6) than IPU and DMT (0.2–0.3% of the initial injected amount in S6) due to their higher desorption. Compared to the previous steps, the pesticide-exportation rate measured during the S8 step may be considered as negligible, even though the four pesticides are present in exported water. This could indicate that renewed flow after a long period of stagnation (i.e. between two drainage seasons in the field) causes a small release of these four pesticides.

3.4 Global pesticide mitigation

In the field, a drainage season is composed of successive periods of high-, low- and zero flow. In order to determine the global pesticide mitigation during a complete drainage season, a mass balance considered the amounts of pesticides injected during the charge steps (S1, S3 and S6), and the amount of pesticides and metabolites exported in water during drainage periods (from S1 to S5 and S8) and adsorbed onto sediment (Fig. 2). Over the 62 days of the experiment, the mitigation ranged from 35.2 to 45.3% for the ditch, and from 7.9 to 14.8% for the pond, with earlier reported mitigation values of 24% for IPU and of 38-67% for BSC (Vallée et al., 2015a). The pesticides from the aqueous phase were exported at outlet mainly during the first steps of HF and LF (S1 to S5, vs. 1.8% for S8). In addition, less than 1% of IPU and DMT metabolites were exported in water at the outlets of both pilots from S1 to S8 (BSC and CYP metabolites were not analysed). From 0.01 to 4.6% of pesticide residues were extracted from sediments; in terms of concentrations, the most recovered was BSC, IPU and DMT were least recovered, and CYP had an intermediate recovery, agreeing with their adsorption coefficients (Gaullier et al., 2018; Vallée et al., 2015a, 2014). We can thus conclude that pesticide mitigation may result from: (i) adsorption onto sediment as previously shown by other authors for BSC (Papaevangelou et al., 2017) and IPU (Durst et al., 2013) (no data for CYP and DMT); (ii) degradation as previously shown for IPU and DMT, (Durst et al., 2013); and (iii) other processes such as plant or biofilm absorption, hydrolysis, photolysis or volatilization, not evaluated in this study but mentioned by (Rönnefahrt et al., 1997; Rose et al., 2008).

4. Conclusions

Our mesocosm experiments demonstrated that pesticide mitigation in CWs is linked to: i) hydrodynamics and in particular flow rates; ii) CW morphology, in this case a ditch and a succession of ponds; and iii) the physico-chemical properties of the pesticide. For the studied flow rates involving similar hydraulic residence times in the two pilots, i.e. high flow and low flow of about 5 h and 24 h, respectively, the ditch seems more effective for mitigating pesticides than the ponds. This is probably due to a lower water depth in the ditch. For both pilots, the mitigation was higher at low flow than at high flow, regardless of the pesticides. In addition to the kinetic aspects of adsorption, again the difference in water depth in each pilot, depending on the flow regime, can be another factor affecting mitigation. At low flow, a higher production of metabolites indicates enhanced degradation, leading to even better mitigation. Finally, no-flow periods led to (almost) total mitigation of both pesticides and their metabolites produced in the water phase.

These laboratory results obtained in controlled conditions highlight how the hydraulic regime that will exist *in situ* and the characteristics of the different drainage episodes will have an impact on the rate of mitigation. The time scale, i.e. long term vs. specific episodes of drainage considered to evaluate the effectiveness of the CWs could thus lead to contrasting results.

Acknowledgements

This research received financial support from the Rhin-Meuse Water Agency, BRGM (French Geological Survey), University of Lorraine, the FEDER-FSE Lorraine et Massif des Vosges (Fonds Européens de DEveloppement Regional – Fond Social Européen) and the Zone Atelier du Bassin de la Moselle. The authors thank the Rhin-Meuse Water Agency and the BRGM for the fellowship. The authors also thank C. Coureau (BRGM, Orléans) for her helpful laboratory work and the farmers R. Cherrier and F.X. Schott (Chambre Régionale d'Agriculture du Grand Est) for field access. Dr. H.M. Kluijver edited the final English version of the MS.

References

Adeosun, J.T., Lawal, A., 2009. Numerical and experimental studies of mixing characteristics in a T-junction microchannel using residence-time distribution. Chemical Engineering Science 64, 2422–2432. https://doi.org/10.1016/j.ces.2009.02.013

Ballabio, D., Consonni, V., 2013. Classification tools in chemistry. Part 1: linear models. PLS-DA. Analytical Methods 5, 3790. https://doi.org/10.1039/c3ay40582f

Blankenberg, A.-G.B., Haarstad, K., Braskerud, B.C., 2007. Pesticide retention in an experimental wetland treating non-point source pollution from agriculture runoff. Water Science & Technology 55, 37. https://doi.org/10.2166/wst.2007.070

Boutron, O., Margoum, C., Chovelon, J.-M., Guillemain, C., Gouy, V., 2011. Effect of the submergence, the bed form geometry, and the speed of the surface water flow on the mitigation of pesticides in agricultural ditches: mitigation of pesticides in agricultural ditches. Water Resources Research 47, n/a-n/a. https://doi.org/10.1029/2011WR010378

Durst, R., Imfeld, G., Lange, J., 2013. Transport of pesticides and artificial tracers in vertical-flow lab-scale wetlands: combined reactive transport of pesticides and tracers. Water Resources Research 49, 554–564. https://doi.org/10.1002/wrcr.20080

Elsaesser, D., Blankenberg, A.-G.B., Geist, A., Mæhlum, T., Schulz, R., 2011. Assessing the influence of vegetation on reduction of pesticide concentration in experimental surface flow constructed wetlands: Application of the toxic units approach. Ecological Engineering 37, 955–962. https://doi.org/10.1016/j.ecoleng.2011.02.003

Fan, L., Reti, H., Wang, W., Lu, Z., Yang, Z., 2008. Application of computational fluid dynamic to model the hydraulic performance of subsurface flow wetlands. Journal of

Environmental Sciences 20, 1415–1422. https://doi.org/10.1016/S1001-0742(08)62542-5

Fernandes, V.C., Domingues, V.F., Mateus, N., Delerue-Matos, C., 2013. Multiresidue pesticides analysis in soils using modified QuEChERS with disposable pipette extraction and dispersive solid-phase extraction: Sample Preparation. Journal of Separation Science 36, 376–382. https://doi.org/10.1002/jssc.201200673

Gaullier, C., Dousset, S., Billet, D., Baran, N., 2018. Is pesticide sorption by constructed wetland sediments governed by water level and water dynamics? Environ Sci Pollut Res 25, 14324–14335. https://doi.org/10.1007/s11356-017-9123-1

Guo C., Cui Y., Dong B., Luo Y., Liu F., Zhao S., Wu H., 2017. Test study of the optimal design for hydraulic performance and treatment performance of free water surface flow constructed wetland. Bioreseource technology 238: 461-471.

Haarstad, K., Braskerud, B.C., 2005. Pesticide retention in the watershed and in a small constructed wetland treating diffuse pollution. Water Science and Technology 51, 143–150.

Holland, J.F., Martin, J.F., Granata, T., Bouchard, V., Quigley, M., Brown, L., 2004. Effects of wetland depth and flow rate on residence time distribution characteristics. Ecological Engineering 23, 189–203. https://doi.org/10.1016/j.ecoleng.2004.09.003

JOCE, 2000. Directive 2000/60/EC of the European Parliament and of the Council of 23 October 2000 establishing a framework for Community action in the field of water policy, L337, 1–73.

Larson, A.C., Gentry, L.E., David, M.B., Cooke, R.A., Kovacic, D.A., 2000. The role of seepage in constructed wetlands receiving agricultural tile drainage. Ecological Engineering 15, 91–104.

Maillard, E., Imfeld, G., 2014. Pesticide Mass Budget in a Stormwater Wetland. Environmental Science & Technology 48, 8603–8611. https://doi.org/10.1021/es500586x

Maillard, E., Lange, J., Schreiber, S., Dollinger, J., Herbstritt, B., Millet, M., Imfeld, G., 2016. Dissipation of hydrological tracers and the herbicide S-metolachlor in batch and continuous-flow wetlands. Chemosphere 144, 2489–2496. https://doi.org/10.1016/j.chemosphere.2015.11.027

Moore, M.T., Bennett, E.R., Cooper, C.M., Smith, S., Shields, F.D., Milam, C.D., Farris, J.L., 2001. Transport and fate of atrazine and lambda-cyhalothrin in an agricultural drainage ditch in the Mississippi Delta, USA. Agriculture, Ecosystems & Environment 87, 309–314.

Moore, M.T., Tyler, H.L., Locke, M.A., 2013. Aqueous pesticide mitigation efficiency of Typha latifolia (L.), Leersia oryzoides (L.) Sw., and Sparganium americanum Nutt. Chemosphere 92, 1307–1313. https://doi.org/10.1016/j.chemosphere.2013.04.099

Papaevangelou, V.A., Gikas, G.D., Vryzas, Z., Tsihrintzis, V.A., 2017. Treatment of agricultural equipment rinsing water containing a fungicide in pilot-scale horizontal subsurface flow constructed wetlands. Ecological Engineering 101, 193–200. https://doi.org/10.1016/j.ecoleng.2017.01.045

Passeport, E., Tournebize, J., Chaumont, C., Guenne, A., Coquet, Y., 2013. Pesticide contamination interception strategy and removal efficiency in forest buffer and artificial wetland in a tile-drained agricultural watershed. Chemosphere 91, 1289–1296. https://doi.org/10.1016/j.chemosphere.2013.02.053

Rönnefahrt I., Traub-Eberhard U., Kördel W., Stein B., 1997. Comparison of the fate of isoproturon in small and large-scale water/sediment systems. Chemosphere 35, 181–189.

Rose, M.T., Crossan, A.N., Kennedy, I.R., 2008. The effect of vegetation on pesticide dissipation from ponded treatment wetlands: Quantification using a simple model. Chemosphere 72, 999–1005. https://doi.org/10.1016/j.chemosphere.2008.04.059

Schultz, R.C., Collettil, J.P., Isenhart, T.M., Simpkins, W.W., Mize, C.W., Thompson, M.L., 1995. Design and placement of a multi-species riparian buffer strip system. Agroforestry Systems 29, 201–226.

Stehle, S., Elsaesser, D., Gregoire, C., Imfeld, G., Niehaus, E., Passeport, E., Payraudeau, S., Schäfer, R.B., Tournebize, J., Schulz, R., 2011. Pesticide Risk Mitigation by Vegetated Treatment Systems: A Meta-Analysis. Journal of Environment Quality 40, 1068. https://doi.org/10.2134/jeq2010.0510

Su, T.-M., Yang, S.-C., Shih, S.-S., Lee, H.-Y., 2009. Optimal design for hydraulic efficiency performance of free-water-surface constructed wetlands. Ecological Engineering 35, 1200–1207. https://doi.org/10.1016/j.ecoleng.2009.03.024

Thackston, E.L., Shields Jr., D., Schroeder, P.R., 1987. Residence time distributions of shallow basins. Journal of Environmental Engineering 113, 1319–1332.

Tournebize, J., Gramaglia, C., Birmant, F., Bouarfa, S., Chaumont, C., Vincent, B., 2012. Co-design of constructed wetlands to mitigate pesticide pollution in a drained catch-basin: a solution to improve groundwater quality. Irrigation and Drainage 61, 75–86. https://doi.org/10.1002/ird.1655

Tournebize, J., Passeport, E., Chaumont, C., Fesneau, C., Guenne, A., Vincent, B., 2013. Pesticide de-contamination of surface waters as a wetland ecosystem service in agricultural landscapes. Ecological Engineering 56, 51–59. https://doi.org/10.1016/j.ecoleng.2012.06.001

Tournebize, J., Chaumont, C., Mander, U., 2017. Implications for constructed wetlands to mitigate nitrate and pesticide pollution in agricultural drained watersheds. Ecological

Engineering 103, 415-425.Vallée, R., Dousset, S., Billet, D., 2015a. Water residence time and pesticide removal in pilot-scale wetlands. Ecological Engineering 85, 76–84. https://doi.org/10.1016/j.ecoleng.2015.09.040

Vallée, R., Dousset, S., Billet, D., Benoit, M., 2014. Sorption of selected pesticides on soils, sediment and straw from a constructed agricultural drainage ditch or pond. Environmental Science and Pollution Research 21, 4895–4905. https://doi.org/10.1007/s11356-013-1840-5

Vallée, R., Dousset, S., Schott, F.-X., Pallez, C., Ortar, A., Cherrier, R., Munoz, J.-F., Benoît, M., 2015b. Do constructed wetlands in grass strips reduce water contamination from drained fields? Environmental Pollution 207, 365–373. https://doi.org/10.1016/j.envpol.2015.09.027

Vandermeeren, P., Baken, S., Vanderstukken, R., Diels, J., Springael, D., 2016. Impact of dry-wet and freeze-thaw events on pesticide mineralizing populations and their activity in wetland ecosystems: A microcosm study. Chemosphere 146, 85–93. https://doi.org/10.1016/j.chemosphere.2015.11.089

Vymazal, J., Březinová, T., 2015. The use of constructed wetlands for removal of pesticides from agricultural runoff and drainage: a review. Environment international 75, 11-20.

Wilson, P.C., Lu, H., Lin, Y., 2011. Norflurazon and Simazine Removal from Surface Water Using a Constructed Wetland. Bulletin of Environmental Contamination and Toxicology 87, 426–430. https://doi.org/10.1007/s00128-011-0380-2

Tables and Figures captions

Table 1: Simulated hydraulic parameters and characteristics of each step (S0 to S8)

Table 2: Water transport parameters of the pilots

Figure 1: Experimental ditch pilot (A) and pond pilot (B) and location of specific zones (SZ) inside the pilots

Figure 2:

Exported rate of dissolved pesticides at outlet during drainage periods, at high flow rate (HF – S1, S2, S4) and low flow rate (LF – S3, S5) and mass balance at the end of experiment (62 days) corresponding of alternating phases of high-, low- and no-flow) for the ditch and the pond

Figure 3:

Distributions of the 16 observations (A) and contributions of the variables (B) obtained from MCA analysis applied on results listed in Table A.5. Based on MCA results, a classification tree (C) obtained with the ascending hierarchical principal component clustering. Groups issued (pond-HF, 1-4; pond-LF, 5-8; ditch-HF, 9-12; ditch-LF, 13-16) from classification tree are used to develop a PLS-DA model (D). These groups correspond also to the intensity migration rate: low (0.6–9%), middle (12.6–20.8%), high (13–33.7%), very high (43.3–50.8%).

Figure 4:

Dissipation of dimethachlor (DMT) and isoproturon (IPU) for the pond and the ditch during the 50-day no flow phase (A) and appearance of their metabolites mono-desmethylisoproturon (MM-IPU) and di-desmethylisoproturon (DD-IPU) (B) and CGA 39981, CGA 42443 and CGA 373464 (C). *(one replicat per pilot, concentrations expressed in mol/L)*

Table 1: Simulated hydraulic parameters and characteristics of each step (S0 to S8)

	Initial State	Charge	Discharge	Charge	Discharge	Discharge	Charge	Stagnation	Discharge
STEP	S0	S1	S2	S3	S4	S5	S6	S7	S8
C_{in} pesticides ($\mu g.L^{-1}$)	0	200	0	200	0	0	200	0	0
Duration step	-	12 h	12 h	36 h	12 h	36 h	12 h	50 d	7 d
Injected ion	-	Cl^-	-	Br^-	-	-	-	-	-
Ditch		**D-HF**		**D-LF**					
Flow rate ($mL.min^{-1}$)	-	6.7 ± 0.2	7.0 ± 0.1	1.8 ± 0.3	6.8 ± 0.1	1.8 ± 0.1	1.8 ± 0.1	-	1.4 ± 0.4
Water level (cm)	0.8	1.5	1.5	1	1.5	1	1	1	1
Volume (L)	0.9	1.7	1.7	1.2	1.7	1.2	1.2	1.2	1.2
HRTn (h)	**-**	**4.3**	**4.0**	**11.0**	**4.2**	**10.7**	**11.1**	**-**	**14.3**
Pesticide/sediment surface contact ($\mu g.cm^{-2}$)	-	0.47	-	0.33	-	-	0.33	-	-
Pond		**P-HF**		**P-LF**					
Flow rate ($mL.min^{-1}$)	-	55.5 ± 1.5	55.1 ± 4.9	8.0 ± 0.2	56.0 ± 0.4	7.9 ± 0.1	8.0 ± 0.3	-	7.4 ± 0.2
Water level (cm)	1.5	3	3	1.5	3	1.5	1.5	1.5	1.5
Volume (L)	4.7	9.4	9.4	4.7	9.4	4.7	4.7	4.7	4.7
HRTn (h)	**-**	**2.8**	**2.8**	**9.8**	**2.8**	**10.0**	**9.8**	**-**	**10.6**
Pesticide/sediment surface contact ($\mu g.cm^{-2}$)	-	0.44	-	0.22	-	-	0.22	-	-

Table 2: Water transport parameters of the pilots

Modality*	t_n (h)	t_{mean} (h)	v_{mean} (cm.h^{-1})	σ	$t_\theta = e_v$	σ^2_Θ	N	λ
D-HF	4.3	4.7	43	2.96	1.1	0.48	2.09	0.57
D-LF	10.9	22.3	9	8.23	2.0	0.57	1.77	0.89
P-HF	2.9	3.9	49	3.63	1.3	1.56	0.64	- 0.74
P-LF	9.8	21.7	10	9.58	2.2	0.96	1.04	0.09

*D-HF, D-LF are the ditch CW with high and low inflow rates, respectively; and P-HF, P-LF are the pond CW with high and low inflow rates, respectively.

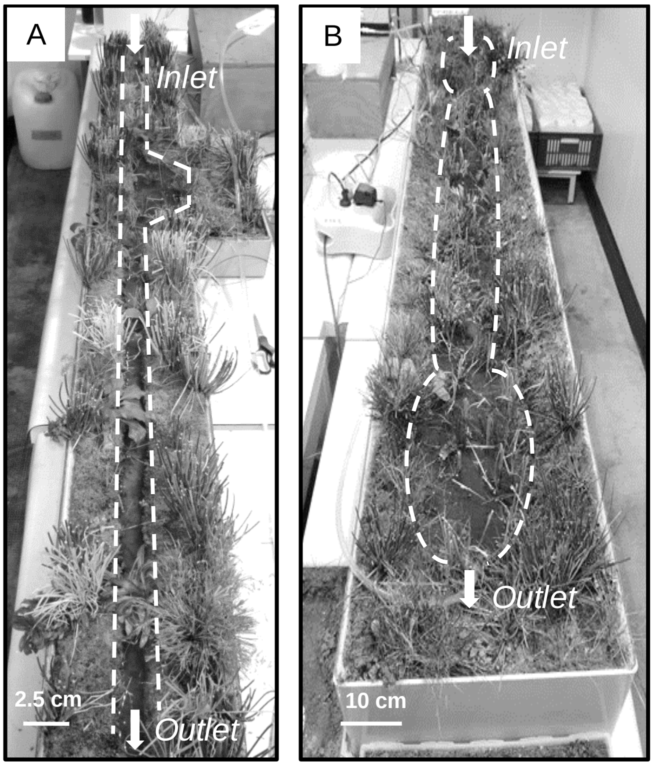

Figure 1

Experimental ditch pilot (A) and pond pilot (B)

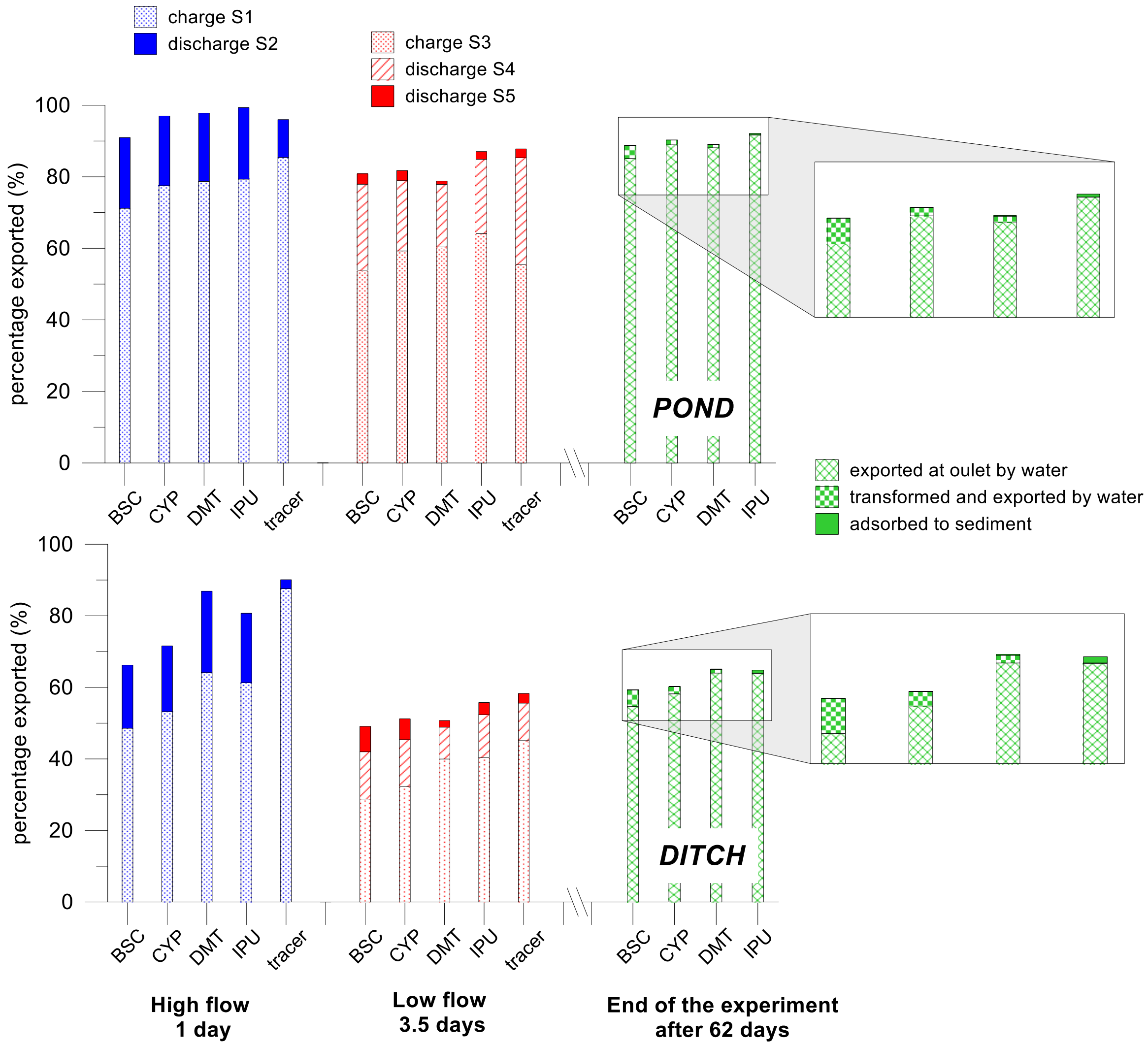

Figure 2

Exported rate of dissolved pesticides at outlet during drainage periods, at high flow rate (HF – S1, S2, S4) and low flow rate (LF – S3, S5) and mass balance at the end of experiment (62 days) corresponding of alternating phases of high-, low- and no-flow) for the ditch and the pond

*The total bromide yield was 102% in the ditch and 98% in the pond, after extraction from plants at the end of the experiment; 44% bromide was recovered from ditch plants and 9% bromide was recovered from pond plants.

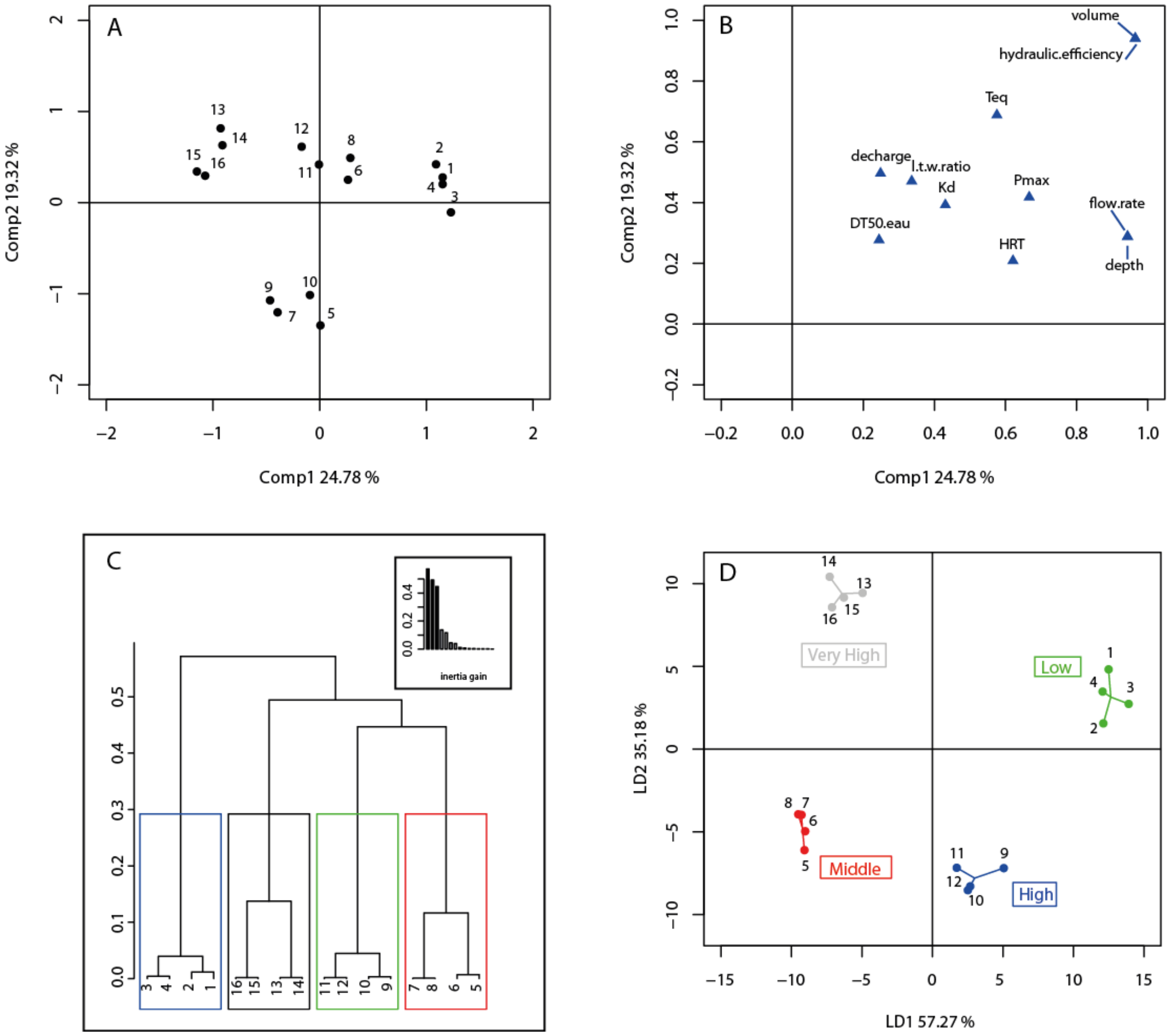
A
Comp1 24.78 %
Comp2 19.32 %
B
volume
hydraulic.efficiency
Teq
decharge
l.t.w.ratio
Kd
Pmax
flow.rate
DT50.eau
HRT
depth
C
inertia gain
D
Very High
Low
Middle
High
LD1 57.27 %
LD2 35.18 %

Figure 3

Distributions of the 16 observations (A) and contributions of the variables (B) obtained from MCA analysis applied on results listed in Table A.5. Based on MCA results, a classification tree (C) obtained with the ascending hierarchical principal component clustering. Groups issued (pond-HF, 1-4; pond-LF, 5-8; ditch-HF, 9-12; ditch-LF, 13-16) from classification tree are used to develop a PLS-DA model (D). These groups correspond also to the intensity migration rate: low (0.6–9%), middle (12.6–20.8%), high (13–33.7%), very high (43.3–50.8%).

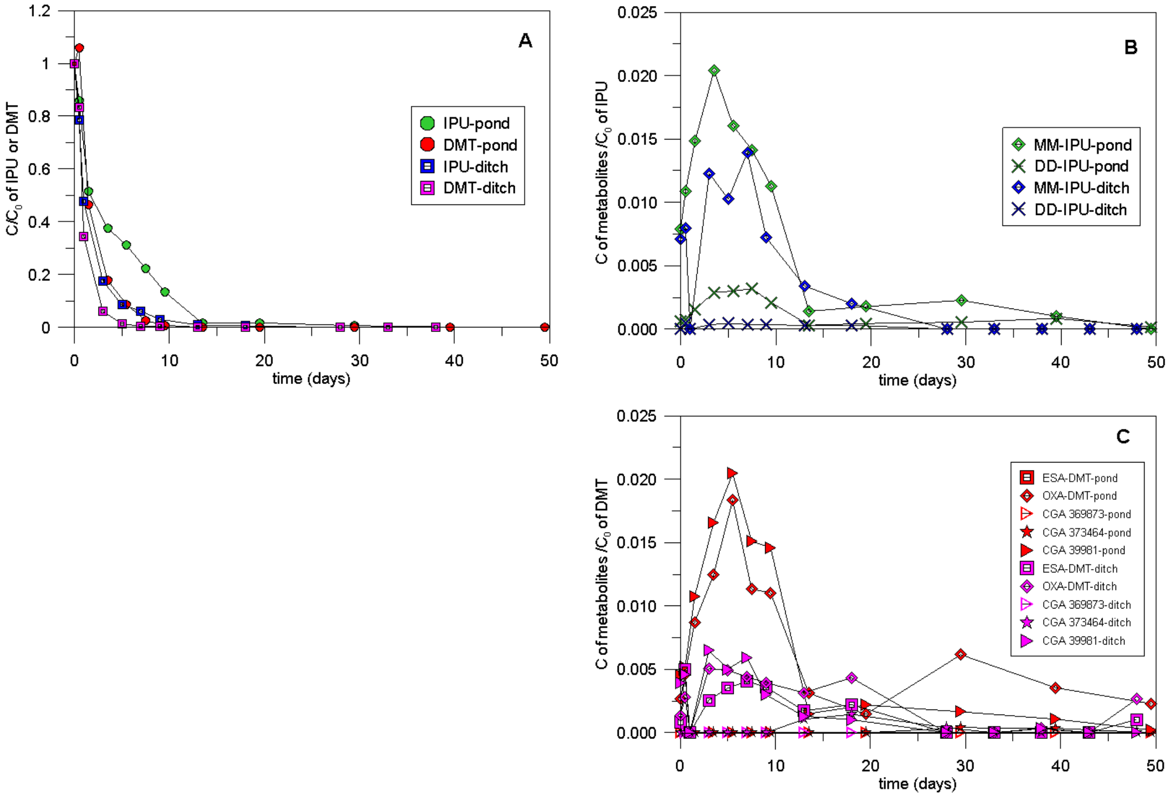

Figure 4

Dissipation of dimethachlor (DMT) and isoproturon (IPU) for the pond and the ditch during the 50-day no flow phase (A) and appearance of their metabolites mono-desmethylisoproturon (MM-IPU) and di-desmethylisoproturon (DD-IPU) (B) and CGA 39981, CGA 42443 and CGA 373464 (C). *(one replicat per pilot, concentrations expressed in mol/L)*

Graphical abstract

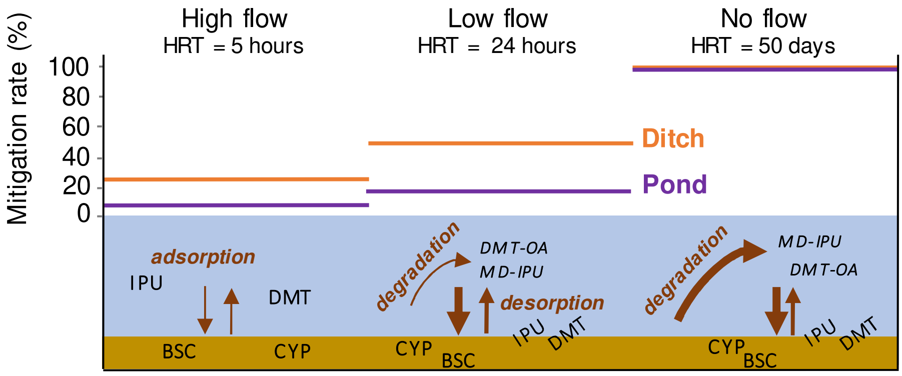

The thicker the arrow, the more important the process